Journal of Controlled Release 162 (2012) 561–567

Contents lists available at SciVerse ScienceDirect

Journal of Controlled Release

journal homepage: www.elsevier.com/locate/jconrel

Enhanced drug delivery capabilities from stents coated with absorbable polymer and crystalline drug

Wenda C. Carlyle [a,*], James B. McClain [a], Abraham R. Tzafriri [b,c], Lynn Bailey [b], Brett G. Zani [b], Peter M. Markham [b], James R.L. Stanley [b], Elazer R. Edelman [c]

[a] Micell Technologies, Inc., 801 Capitola Drive, Suite 1, Durham, NC 27713-4384 USA
[b] CBSET, Inc., Concord Biomedical Sciences & Emerging Technologies, 500 Shire Way, Lexington Technology Park, Lexington, MA 02421 USA
[c] Massachusetts Institute of Technology, 77 Massachusetts Avenue (E-25-438), Cambridge, MA 02139 USA

ARTICLE INFO

Article history:
Received 8 May 2012
Accepted 7 July 2012
Available online 16 July 2012

Keywords:
Stent
PLGA
Crystalline
Sirolimus
Modeling
Pharmacokinetic

ABSTRACT

Current drug eluting stent (DES) technology is not optimized with regard to the pharmacokinetics of drug delivery. A novel, absorbable-coating sirolimus-eluting stent (AC-SES) was evaluated for its capacity to deliver drug more evenly within the intimal area rather than concentrating drug around the stent struts and for its ability to match coating erosion with drug release. The coating consisted of absorbable poly-lactide-*co*-glycolic acid (PLGA) and crystalline sirolimus deposited by a dry-powder electrostatic process. The AC-SES demonstrated enhanced drug stability under simulated use conditions and consistent drug delivery balanced with coating erosion in a porcine coronary implant model. The initial drug burst was eliminated and drug release was sustained after implantation. The coating was absorbed within 90 days.

Following implantation into porcine coronary arteries the AC-SES coating is distributed in the surrounding intimal tissue over the course of several weeks. Computational modeling of drug delivery characteristics demonstrates how distributed coating optimizes the load of drug immediately around each stent strut and extends drug delivery between stent struts. The result was a highly efficient arterial uptake of drug with superior performance to a clinical bare metal stent (BMS). Neointimal thickness (0.17 ± 0.07 mm vs. 0.28 ± 0.11 mm) and area percent stenosis ($22 \pm 9\%$ vs. $35 \pm 12\%$) were significantly reduced ($p<0.05$) by the AC-SES compared to the BMS 30 days after stent implantation in an overlap configuration in porcine coronary arteries. Inflammation was significantly reduced in the AC-SES compared to the BMS at both 30 and 90 days after implantation.

Biocompatible, rapidly absorbable stent coatings enable the matching of drug release with coating erosion and provide for the controlled migration of coating material into tissue to reduce vicissitudes in drug tissue levels, optimizing efficacy and reducing potential toxicity.

1. Introduction

Coronary arterial drug-eluting stent (DES) significantly improved outcomes and reduced the need for additional interventions. Millions have benefited from this technology and the knowledge gained from extensive use of these products has provided insights into aspects of the technology critical to therapeutic effectiveness. Essential attributes include use of an underlying balloon delivery catheter optimized for flexibility and placement accuracy; a stent platform that minimizes strut thickness and a drug-eluting coating that optimizes local antiproliferative therapy with coating compositions that minimize any inflammatory response.

Several lessons are emerging as dominant in the DES era – in particular the role of stent design and geometry, and the material and coating characteristics. Thinner struts, for example, reduce intimal hyperplasia and thrombotic potential, improving clinical outcomes [1,2]. Less clear is how to formulate the coating to optimize drug delivery and device biocompatibility.

Restenosis is most likely in the months immediately following stent placement [3]. Injury to the vessel wall is a triggering event and a subsequent inflammatory response will continue to encourage neointimal hyperplasia and vascular restenosis. Any component of the DES that exacerbates the inflammatory response or delays healing of the vessel will prolong the risk of adverse events such as late stent thrombosis. Although most polymer coatings have some inflammatory potential [4], the coating is needed to secure the drug to the device during delivery and to control release of the drug after implantation.

* Corresponding author. Tel.: +1 715 455 2766 (office), +1 203 300 4277 (mobile).
E-mail addresses: wenda.carlyle@sbcglobal.net (W.C. Carlyle), jmcclain@micell.com (J.B. McClain), rtzafriri@cbset.org (A.R. Tzafriri), lbailey@cbset.org (L. Bailey), bzani@cbset.org (B.G. Zani), pmarkham@cbset.org (P.M. Markham), bstanley@cbset.org (J.R.L. Stanley), ere@mit.edu (E.R. Edelman).

0168-3659/$ – see front matter © 2012 Elsevier B.V. All rights reserved.
doi:10.1016/j.jconrel.2012.07.004

Currently marketed DES often provides short-term delivery of the therapeutic drug and a much longer (usually permanent) presence of the potentially inflammatory polymer coating. Absorbable polymer coatings that fully degrade and leave a bare metal stent provide the opportunity for more optimum long-term biocompatibility [5].

Drug release from current DES coatings is controlled by the rates of water imbibition into the polymer coating, subsequent dissolution of the drug and diffusion of soluble drug out of the polymer matrix [6]. Release is therefore exponential with an initial burst phase corresponding to rapid dissolution of surface drug [7]. This burst release may present the artery with more drug than it can retain resulting in measurable systemic drug levels [8]. The ensuing exponential decay of drug delivery means that drug release is constantly declining such that the interval during which optimal drug dosing is achieved may be very limited.

A common concern is that stent-based drug delivery patterns tend to track the structure of the stent scaffold [9–11], and that this might result in suboptimal dosing between the struts and excessive dosing adjacent to stent struts. We used in vivo and computational models to determine whether a DES product could reduce the peaks and valleys in drug concentration by creating a formulation whose coating could be deployed away from the strut to more uniformly distribute drug through the vessel wall. We further sought to determine if a coating material deployed in this manner could be made to absorb rapidly relative to the duration of drug elution without eliciting a significant inflammatory response.

2. Methods

2.1. AC-SES

An absorbable coating-sirolimus-eluting stent (AC-SES: MiStent® Sirolimus Eluting Absorbable Polymer Coronary Stent System, Micell Technologies, Inc., Durham, NC) was based on a cobalt-chromium stent platform (GENIUS® Magic, Eurocor GmbH, Bonn Germany) [12] The stent has thin 0.0025 inch struts. The coating consists of sirolimus combined with an absorbable polymer, poly(lactide-*co*-glycolic acid) (PLGA). Unique to this DES is the combination of the absorbable polymer and drug components using a dry powder electrostatic coating process. This product is not currently approved for commercial distribution.

2.2. Stent coating

A detailed description of the stent coating procedure can be found in the supplemental materials and is outlined in Fig. 2.

2.3. SEM imaging

Samples were sputter coated with platinum for 1.5 min to achieve a coating of approximately 15 nm. Imaging was performed at Evan Analytical Laboratories (Raleigh, NC) on a Hitachi S-4700 Field Emission scanning electron microscope. Images were acquired ranging from 35× to 5000× magnification.

2.4. Drug stability measurements

Drug stability assessment under simulated use conditions was performed at Eurofins Medinet, Inc. (Aurora, CO). For these experiments drug stability within the AC-SES containing crystalline sirolimus was compared to sirolimus stability in a standard, commercially available DES product that consists of amorphous drug in a permanent polymer [7]. A total of six Cypher® DES controls (Cordis, Miami Lakes, FL) and twelve AC-SES were used for the stability assessment. The coating was dissolved and extracted from three controls and six AC-SES test articles by addition of 2 ml acetone:methanol (50:50) at baseline for reference to incubated stents. The remaining stents were incubated for 14 days in serum supplemented cell culture media at 37 °C. At the end of this period, the stents were removed and their coatings extracted as described above. Extracted samples were stored at −80 °C such that quantification was performed simultaneously on all samples. A fully validated method employing HPLC linked to tandem mass spectrometry (HPLC-MS/MS) was used for analysis of sirolimus and degradants. The analysis was performed using an API 4000 Triple Quad Mass Spectrometer (AB Sciex Instruments) paired to a Waters Acquity HPLC system. Data were captured and analyzed within the Analyst 4.2.1 software package. Sirolimus content was analyzed to quantify relative amount of parent drug and primary degradants.

2.5. Flow loop studies

An *in vitro* flow loop consisting of a 60 cm long, 3.35 mm diameter Silastic® tube was used to create controllable, vessel-like flow conditions as determined by velocity, pressure and wall shear stress. Individual AC-SES were deployed inside the flow loop and expanded at 8 bar to ensure complete apposition to the tubing wall. The system was filled with a 0.01 M PBS/7.5% BSA solution at 37 °C. The loops were loaded into the flow system and exposed to controlled coronary artery-like flow (pulsatile, 15 dyn/cm^2) at 37 °C for 4 h, 1, 3, 7 and 14 days. Immediately following the specified run time, the loops were removed, emptied, flushed with PBS to remove non-adherent debris and stored for subsequent imaging. AC-SES samples were kept in the tube and immersed in PBS, then photographed macroscopically under a stereoscope employing dark field illumination to visualize the coating.

2.6. Porcine coronary artery implants

Porcine coronary artery implants and subsequent SEM, histopathology and histomorphometry analyses were performed at CBSET, Inc. (Lexington, MA) using laboratory standard operating procedures.

For histopathology and histomorphometry, Yucatan mini-swine were implanted with AC-SES and/or Vision® bare metal stents (BMS, Abbott Vascular, Santa Clara, CA) for 3, 30 or 90 days. Stents were deployed in porcine coronary arteries at a balloon:artery ratio of approximately 1.13:1 in either a single stent configuration or in an overlapping stent configuration using same-stent pairs (AC-SES or BMS) overlapped by approximately 50%. Eight single stents or stent pairs were used for each stent type and time point.

For pharmacokinetic analysis, Yucatan mini-swine were implanted with AC-SES for 1, 3, 7, 14, 21, 30, 45, 60, 90 and 180 days (a minimum of six stents per time point). One AC-SES was deployed in one porcine coronary artery per pig at a balloon:artery ratio of approximately 1.15:1.

2.7. Histology and morphometry

At the termination of the in-life portion of the study, porcine hearts were perfusion fixed at 100 mm Hg. Fixed, stented vessels were dissected from the myocardium, sectioned and stained with hematoxylin and eosin as well as Verhoeff's tissue elastin stain. Light microscopy was used to score the tissue for histopathological variables as described in Supplemental Materials. Scoring was performed by a pathologist (co-author J.R.L.S.) in a blinded fashion. Inflammation and injury were scored on a per strut basis and the average was calculated per plane and per stent.

Quantitative morphometric analysis was performed on the histological sections from each stented artery using standard light microscopy and computer-assisted image measurement systems (Olympus MicroSuite Biological Suite). Lumen area, IEL bounded area, stent area and EEL bounded area were all measured directly. From these measurements, all other morphometric parameters were calculated.

2.8. Pharmacokinetic analysis

Hearts were removed and the stented vessels were dissected from the myocardium including vessel proximal and distal to the stented segment. The stent was cut longitudinally and tissue was removed from the stent. Drug content was assessed separately from the stent and the tissue surrounding the stent. During manual separation of the stent from the arterial tissue, tissue embedded coating deposits were retained with the tissue fraction and account for additive drug in the measured tissue concentrations seen during analysis of drug content. Blood levels were also measured from a separate set of pigs and include additional time points minutes to hours after implantation. Concentration of drug in tissue, blood and on stents was determined using a validated HPLC-MS/MS method using an Agilent 1200 LC system paired to Applied Biosystems API5500 MS with Analyst 1.5 software.

2.9. Data acquisition and analysis

Data are presented as mean ± standard error. For selected continuous data, if the assumptions of normality and homogeneity of variance were met, treatment differences were assessed by group t-test. If normality or homogeneity of variance were not met, treatment differences were assessed by Mann–Whitney Rank Sum test. For multiple comparisons, treatment differences were assessed by a Kruskal–Wallis One Way Analysis of Variance on Ranks. For all statistical tests, the null hypothesis of no difference was only rejected if the value of the calculated statistic was less than 0.05 ($p<0.05$).

2.10. Computational studies

We developed a 2D computational pharmacokinetics model to evaluate the influence of coating deployment on drug distribution patterns relative to a representative pair of rectangular struts (Fig. 1). Strut dimensions (60×80 μm) and inter-strut separation (1.35 mm) were based on AC-SES dimensions and the initial polymer coating idealized as 5-μm thick conformal layer. Motivated by morphometry micrographs (Fig. 5), coating deployment was modeled as a vertical and horizontal migration of coating segments. Drug elution was implemented as a prescribed constant flux at the interfaces between coating and tissue (based on early in vivo release kinetics). Drug transport in the tissue was assumed to be governed by a constant isotropic diffusion coefficient and bimolecular binding [13] to nonspecific tissue sites and to intracellular FKBP12 [14], using published parameter estimates (Table S1, online supplement). Luminal and periadventitial washout were accounted for by applying perfect sink boundary conditions at these interfaces [9,15]. In accordance with the periodicity of the stent geometry, proximal (inlet) and distal (outlet) boundaries of the computational geometry were treated as perfect insulators (e.g. symmetry boundary conditions).

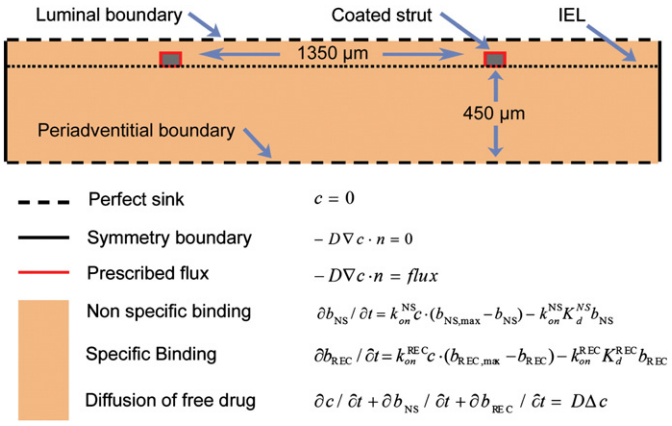

Fig. 1. Scaled schematic representation of the 2D computational domain of a tissue embedded strut pair apposed to the internal elastic lamina (IEL). Depicted here is the baseline case of conformable strut-adherent coating. Notations: t - time since stent implantation; n - unit normal; c - concentration of free drug, b_{NS} and b_{REC} - concentrations of, respectively, non specific - (NS) and receptor - (REC) bound drug; $b_{NS,max}$ and $b_{REC,max}$ - concentrations of NS binding sites and receptors; k_{on}^{NS} and k_{on}^{REC} - respective binding on-rate constants, K_d^{NS} and K_d^{REC} - respective equilibrium dissociation constants; D - drug diffusion coefficient in arterial tissue (for parameter values see Table S2, Supplemental Materials).

While modeling provides important insights into the kinetics of drug dissociating from the stent it does not directly quantify how much of the drug released is free relative to that still embedded in coating deposits.

3. Results

3.1. Stent coating and stability

The electrostatic coating process results in the deposition of dry powder, crystalline sirolimus onto the stent surface. This is a solvent-free coating process further differentiated by the use of supercritical fluid technology to apply the polymer component [16]. The average crystal particle size of the drug deposited on the stent surface is 2.7 μm with all particles between 1.0 and 10 μm.

Because the drug is never dissolved in solvent the crystal structure is maintained during application of the coating. Drug and polymer are layered onto the stent and each layer is sintered to fuse the coating into a smooth, conformal, well-adhered film (Fig. 2).

Maintaining the crystalline structure of sirolimus within the coating conferred enhanced drug stability. When coated stents were incubated in serum-supplemented cell culture medium at 37 °C, a reduced percentage of degradants relative to parent drug were found in the stent coatings containing crystalline sirolimus compared to a standard stent coating containing approximately the same amount of sirolimus but in amorphous form. The levels of the major sirolimus degradant two weeks after incubation under simulated use conditions rose from a baseline value of 0.1% ± 0.06% to 11.0% ± 1.0% in stents coated with

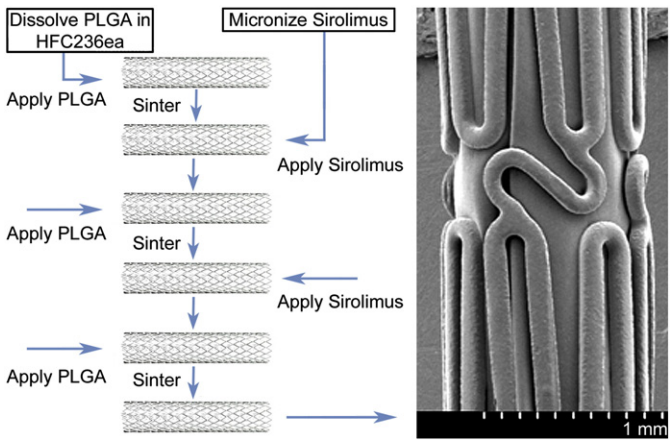

Fig. 2. Sequential addition of PLGA and micronized sirolimus is followed by sintering that fuses the layers into a smooth, conformal stent coating.

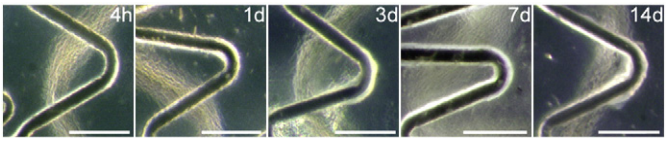

Fig. 3. AC-SES stents were incubated in a flow loop for up to 14 days and imaged through the clear silastic tubing with dark field microscopy. Coating spread is seen as a broadening of the white areas surrounding the stent struts. Bars represent 500 μm.

amorphous sirolimus. In stents with coatings incorporating crystalline sirolimus the increase in degradant was much reduced. Here the relative amount of degradant increased from 0.5%±0.5% to 3.2%±1.8%). This 3.4 fold lower value of relative degradant after two weeks of incubation represents a statistically significant reduction in sirolimus degradation ($p<0.05$).

3.2. Coating dispersion and drug delivery

Absorbable coatings behave differently compared to strut-adherent durable polymer coatings. The structure of the absorbable coating enables the polymer material to soften and spread after implantation. Fig. 3 shows results from flow loop studies performed to visualize coating changes in the AC-SES under simulated implant conditions employing pulsatile flow. In this study, changes in coating morphology were evaluated up to 14 days and the coating was found to become swollen and to gradually spread away from the stent strut in a uniform manner. No evidence of delamination was found to occur.

The flow loop studies involved a simplified, cell-free preparation where serial visualization of changes in coating morphology is possible. In the flow loop studies, the stent is deployed against the wall of a flexible polymer tube and fluid is pumped through the tubing to hydrate the coating. These studies differ from *in vivo* implantation into a coronary artery, because in the *in vivo* situation the stent coating is in direct contact with tissue. As the coating degrades and becomes more porous, cells within the neointima can intercalate into the coating and cause the coating to separate from the stent struts. Most polymer materials, including PLGA, are labile and susceptible to dissolution in the fluids used for histological processing of stented tissue sections. The location, size and shape of the polymer coating in histology sections is witnessed rather as the "negative image" of a space occupying mass. Fig. 4 illustrates this phenomenon and provides evidence of coating spread or deposition in the intima 30 days after AC-SES implantation into porcine coronary arteries.

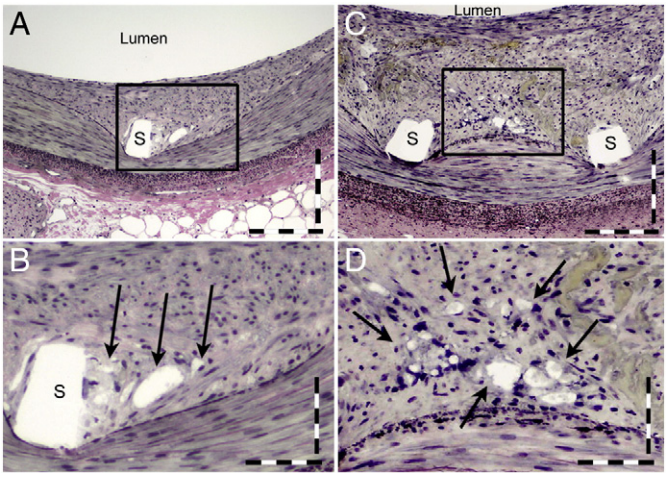

Fig. 4. Data from preclinical studies evaluating AC-SES after 30 day implant in the porcine coronary implant model. The square-shaped clear spaces represent the stent strut (S) location though the actual strut was lost during processing of the histology slides. In each panel, distinct, irregularly shaped clear spaces (B, D: black arrows) represent areas previously occupied by coating that has been lost during processing. Coating can be seen to have spread into the surrounding neointima either close to the strut (A, B) or relatively distant (C, D). Bars represent 200 μm (A, C) and 75 μm (B, D).

The spreadable coating reduces the load of drug immediately around the stent strut and extends polymer/drug coating from the strut. The coating deposits contain drug still locked in a crystalline lattice combined with the softened PLGA polymer. Thus, the area of drug delivery is increased beyond the immediate vicinity of the stent strut. Modeling of this phenomenon demonstrates that at small migration distances deposition is enhanced due to greater surface area of elution. Above some threshold distance, deposition is also enhanced by saturation of binding sites that are otherwise free in the strut-adherent case (Fig. 5).

3.3. Rapid coating absorption

By 90 days after implantation there is no further evidence of coating deposits suggesting near complete absorption of coating by that point (Fig. 6). Following implantation of any stent coated with an absorbable polymer, the thickness of the strut and its associated coating will vary over time as the polymer absorbs. After 90 days, the absence of stent coating leaves the struts (represented as "S" and seen as the square shaped clear space) at their bare metal dimensions.

3.4. Controlled and consistent drug release

When drug is locked in a crystalline lattice within the stent coating it must dissociate from the crystal before diffusion through the polymer and elution from the coating can commence. When drug solubilization is rate-limiting, the rate of drug elution will remain relatively constant over time exhibiting release kinetics that are far less concentration gradient-dependent than classic diffusion-based drug delivery systems. Published theoretical analyses [17] predict that dissolution controlled release of crystalline drugs should display zero order kinetics elution after a negligibly small initial burst. Indeed the AC-SES displays a virtual absence of an initial burst of drug release (Fig. 7). The stent containing crystalline sirolimus releases its drug in a near linear fashion over several weeks. Within 45–60 days the stent is essentially free of sirolimus (less than 3% remains at the 45 day time point).

3.5. Drug transfer to tissue

In vivo release of drug from the stent is complete within 45–60 days after implantation into porcine coronary arteries (Fig. 7, open circles). The average release rate amounts to ~3 μg/day of sirolimus from a 3.0×15 mm stent. Control over sirolimus release results in efficient drug transfer to and deposition within the arterial tissue (Fig. 7, closed circles).

Early after implant the coating is still firmly attached to the stent as demonstrated in the flow loop studies. During this time, the vast majority of drug remains in the coating adhered to the stent. Some drug is seen in tissue and likely consists largely of free drug released from the coating. As time goes on, drug still trapped in coating that has dissociated from the stent (Fig. 4) will represent an increasing fraction of the measured amount of drug in tissue. We hypothesize that by day 30 polymer degradation progresses to the point where coating adhesion begins to appreciably decline so that a much greater percentage of coating can detach from the stent and disperse into tissue where it is quantified as "arterial drug concentration." Between 45–60 days, all the coating is released from the stent. From that point on, the tissue levels will fall as drug is slowly cleared from the site and there is no residual sirolimus left on the stent to supply additional drug.

3.6. Biocompatibility throughout the period of polymer absorption

Despite the sustained presence of sirolimus after implantation of the AC-SES in porcine coronary arteries, endothelialization was not

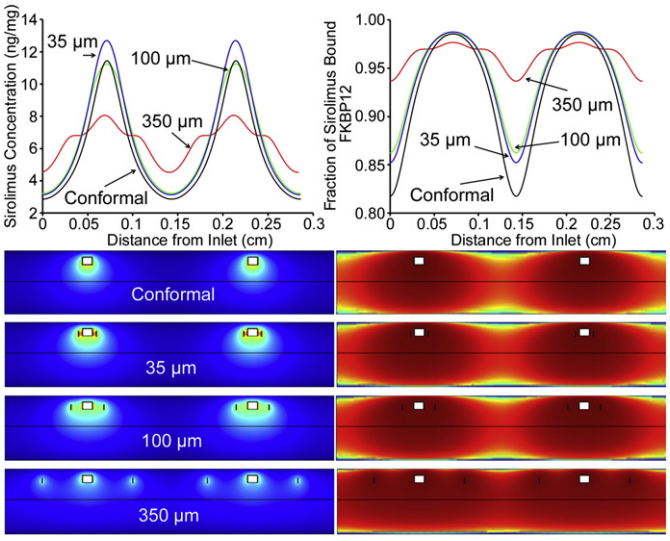

Fig. 5. Modeling of drug delivery characteristics based on the assumptions that the coating moves lateral relative to the stent strut, that both struts have the same amount of coating migration and that (in this example) approximately 30% of the coating migrates. All color schemes are uniform (0–1 for bound receptors; 0–40 ng/mg for deposited drug). "Conformal" refers to strut-adherent coating and the numbers 35, 100 and 350 represent relative distances from the stent strut.

different from the control BMS and was complete by 30 days after implantation (Table 1).

Implantation of this unique stent system coated with crystalline sirolimus and PLGA into porcine coronary arteries generated a benign tissue response characterized by the expected increase in fibrin deposition and some minimal mineralization (Figs. 4 and 6). The porcine coronary artery implant model used was a safety model involving minimal overstretch. This non-overstretch model typically shows little neointimal hyperplasia except in the presence of additional stimuli such as pro-inflammatory stent coatings. Following single stent placement in this model, the AC-SES resulted in a tissue response similar to that seen following placement of the control BMS. When this model is challenged, however, with placement of two overlapping stents, then even bare metal stent implantation will trigger an increased tissue response [18,19]. Implantation of overlapping AC-SES resulted in reduced inflammation and neointimal hyperplasia compared to implantation of overlapping bare metal control stents at 30 and 90 days after implantation (Figs. 8 and 9, Table 1).

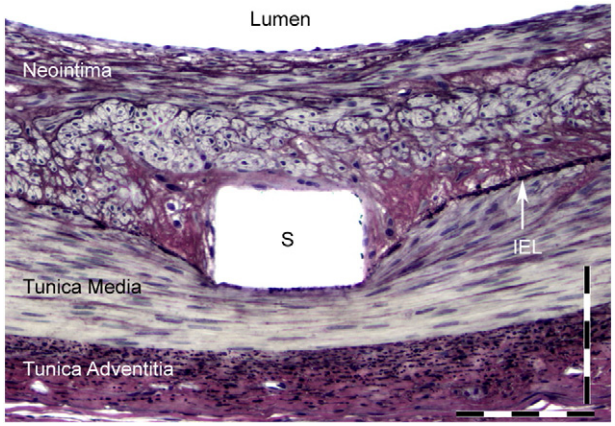

Fig. 6. After 90 days of implantation, the coating is largely absorbed as is evidenced by the resolution of clear areas representing space-occupying coating. Bars represent 100 µm.

4. Discussion

The principal advantage of an absorbable stent coating has been viewed as its temporary residence time such that any inflammatory potential brought about by its presence is of limited duration. We show here that additional benefit can be derived from the ability of the absorbable coating to soften, spread and migrate into surrounding tissue. This deployment of the coating provides more uniform drug distribution and the ability to saturate binding sites farther from the stent struts. Drug therapy is mediated by this binding to target receptors and it is the amount of drug bound to these receptors at any given time that dictates drug effectiveness, not the total amount of drug present either on the stent or in the artery. As vessel injury from balloon delivery of the stent occurs all along the vessel wall, anti-restenotic therapy is optimized by receptor binding both at and between stent struts. Equally important to the expanded area of drug delivery is the consequent reduction in peak drug concentrations in the immediate vicinity of the stent struts. High concentrations of drug may result in focal regions of tissue toxicity and vessel thrombogenicity [20].

The crystalline nature of the drug load in the AC-SES coating provides additional control over drug delivery. The drug locked in crystalline particles does not diffuse within the coating and after implantation of the AC-SES far less drug is available for immediate release. This eliminates the burst of drug release seen otherwise with most commercially available strut-adherent matrix DES products. The burst seen with other products within minutes to hours after stent implantation is equivalent to delivery of a large bolus of drug that is more than the artery can retain [21] and much of the excess drug is washed away in the systemic circulation. In contrast, systemic sirolimus levels in the porcine coronary implant model following implantation of the AC-SES containing crystalline sirolimus remain below the level of quantification (<0.1 ng/ml) at all times [22]. Release of a large burst of drug soon after stent implantation at a time when there is little or no neointima separating the stent from the endothelium may cause additional endothelial damage and dysfunction [23].

Drug that is part of a crystalline structure must overcome a high activation energy barrier to dissociate from that crystal before it can diffuse away from the coating. This means that the dissociation/dissolution reaction becomes the rate-limiting step in drug delivery rather than the diffusion of drug from the stent [24]. With dissociation from the crystalline lattice controlling the rate of drug release, a more consistent rate of

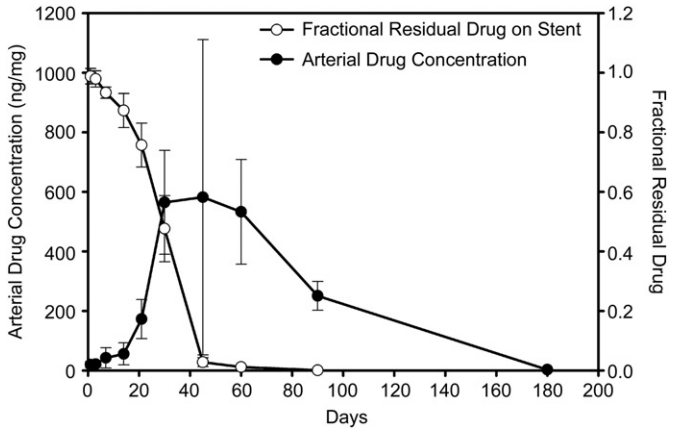

Fig. 7. Drug release was shown to be complete within 45–60 days after stent implantation into porcine coronary arteries. The average daily release rate amounts to approximately 3 µg of sirolimus from a 3.0×15 mm stent. Arterial levels of drug were quantified from arterial tissue surrounding the stented segment. Each data point represents the average from quantification of six stents. Data are presented as ± standard error.

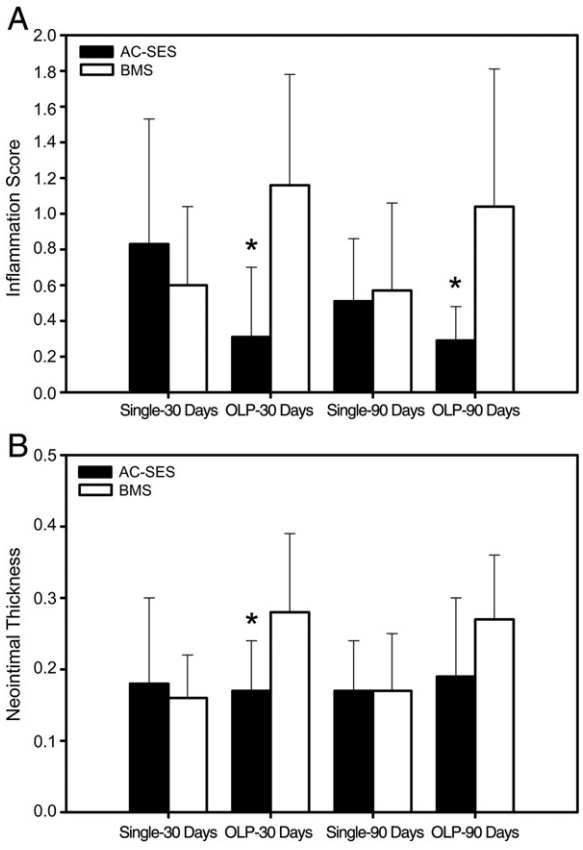

Fig. 8. Comparison of AC-SES with BMS at 30 and 90 days after implant under conditions of single or overlapping (OLP) stent configurations. Inflammation was scored as described in Table 1. Neointimal thickness was calculated by subtracting the lumen diameter from the internal elastic lamina diameter and dividing by two. Data are presented as ± standard error. * $p<0.05$.

drug release can be maintained regardless of the amount of drug remaining in the coating.

The slow, consistent release of drug from the AC-SES sustains drug release for an extended period. This allows for delivery of drug throughout the period of polymer absorption. As sirolimus is both an anti-inflammatory agent [25,26] as well as an anti-proliferative drug, its presence can counteract any tissue reaction from generation of polymer degradation products during the period of polymer absorption. Ideally, sirolimus should be delivered from the DES at a consistently therapeutic dose that is sufficient to limit intimal hyperplasia without delaying the re-endothelialization of the vessel critical to healing. The AC-SES appears to accomplish this goal as endothelialization after implantation was not different from that of a BMS. By balancing drug delivery with the relatively rapid absorption of the polymer within a 90-day period the AC-SES optimizes therapy and allows for healing without concerns of late vascular events due to lingering effects of stent coating.

The use of this rapidly absorbable PLGA formulation adds a new dimension to coated stents, the potential for a deployable coating. The time-dependent changes in PLGA stent-coating morphology and integrity have recently been described [27] based on *in vitro* and *in vivo* degradation studies analyzed by a variety of techniques including light microscopy, gel permeation chromatography, weight loss, field-emission environmental scanning electron microscopy (SEM) and standard SEM. After implantation, any bioabsorbable polymer absorbs moisture from the surrounding tissue and begins to swell. Hydration leads eventually to polymer degradation by the process of hydrolytic cleavage of the ester bonds. Polymer molecular weight decreases relatively rapidly as bonds are broken, mass loss occurs more slowly. These data demonstrate a homogenous degradation process in which the coating maintains its integrity and strong adhesion to the strut during the entire degradation process. Implantation of the AC-SES in a flow loop resulted in a similar finding of PLGA swelling and spread.

In these studies no delamination was observed; however it is important to note that the *in vivo* degradation studies performed by Xi et al. utilized a PMMA chamber to exclude cells from making contact with the coated stent after subcutaneous implantation. Direct contact with cells such as occurs after coronary artery implantation will lead eventually to cell infiltration into the degrading coating and this will serve to separate the coating from the stent struts. Similar to the benefit derived from a more uniform tissue distribution of sirolimus, spreading of polymer in the tissue may facilitate absorption and dilute the local accumulation of degradation products.

Coating dispersion will only be useful from a drug delivery perspective if the time course of morphological changes is matched by the time course of drug delivery. Other known stents coated with absorbable polymers have a relatively prolonged degradation such that movement of the polymer is likely to occur only after several months [28]. At the same time, as described above, the drug within these coatings is in an amorphous form that is released from the stent relatively quickly, often losing much of the drug load in a burst within minutes to hours after implantation. In these cases, by the time the polymer coating disperses into the tissue, there is no longer sufficient drug remaining in the coating to provide enhanced drug delivery.

In conclusion several aspects of the AC-SES lend themselves to improved drug delivery. The inclusion of crystalline rather than amorphous drug in the coating results in consistent drug release kinetics that lack an initial burst. A deployable polymer coating reduces the vicissitudes in drug levels and broadens that area of arterial wall with binding site occupancy. The polymer coating absorbs rapidly leaving a bare metal stent with fewer concerns about long-term biocompatibility.

Table 1
Comparison of AC-SES and BMS at 30 days in porcine coronary arteries.

Parameter	AC-SES	BMS
Endothelialization	Complete	Complete
Neointimal area	1.38 mm ± 0.44 mm*	2.26 mm ± 0.82 mm
Area % stenosis	22% ± 9% *	35% ± 12%
Neointimal thickness	0.17 mm ± 0.07 mm*	0.28 mm ± 0.11 mm

* $p<0.05$.

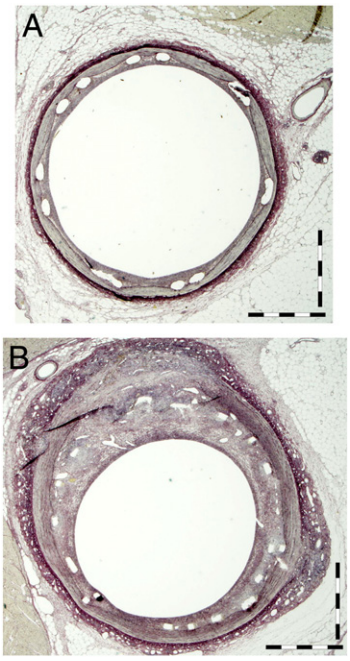

Fig. 9. Day 30 AC-SES (A) Vision BMS (B) overlapping stents. Bars represent 1 mm.

The resulting composite product reduces intimal hyperplasia compared to a bare metal stent in a physiologically challenging setting of overlapping stents.

Conflict of interest statement

Drs. Carlyle and Edelman are paid consultants of Micell Technologies, Inc. and Dr. Edelman has a financial interest in the company. Dr. McClain is an employee of Micell Technologies. Co-authors Tzafriri, Bailey, Zani, Markham and Stanley are employees of the contract research laboratory CBSET that was hired to perform the animal and computational studies.

Role of the funding source

This study was supported by funds from Micell Technologies, Inc. (Micell), Durham, NC and from NIH R01 GM49039 to ERE. Employees from Micell provided input into the study design and editorial input into the writing of reports. Data collection, analysis and interpretation were all performed independent of input from Micell. The decision to submit the paper for publication came from joint discussions between Micell management and all authors.

Acknowledgments

The Authors are indebted to Philip Seifert and Jordi Martorell for their help with the microscopy and flow loop studies, to Gee Wong for his help with the histomorphometry and quantitative analysis, and to Greg Kopia for his thoughtful analysis of the pharmacokinetic data.

Appendix A. Supplementary data

Supplementary data to this article can be found online at http://dx.doi.org/10.1016/j.jconrel.2012.07.004.

References

[1] A. Kastrati, J. Mehilli, J. Dirschinger, F. Dotzer, H. Schuhlen, F.-J. Neumann, M. Fleckenstein, C. Pfafferott, M. Seyfarth, A. Schomig, Intracoronary stenting and angiographic results: strut thickness effect on restenosis outcome (ISAR-STEREO) trial, Circulation 103 (2001) 2816–2821.
[2] J. Pache, A. Kastrati, J. Mehilli, H. Schuhlen, F. Dotzer, J. Hausleiter, M. Fleckenstein, F.J. Neumann, U. Sattelberger, C. Schmitt, M. Muller, J. Dirschinger, A. Schomig, Intracoronary stenting and angiographic results: strut thickness effect on restenosis outcome (ISAR-STEREO-2) trial, J. Am. Coll. Cardiol. 41 (8) (2003) 1283–1288.
[3] D.R. Holmes Jr., State of the art in coronary intervention, Am. J. Cardiol. 91 (3A) (2003) 50A–53A.
[4] R.A. Byrne, M. Joner, A. Kastrati, Polymer coatings and delayed arterial healing following drug-eluting stent implantation, Minerva Cardioangiol. 57 (5) (2009) 567–584.
[5] G. Nakazawa, A.V. Finn, F.D. Kolodgie, R. Virmani, A review of current devices and a look at new technology: drug-eluting stents, Expert Rev. Med. Devices 6 (1) (2009) 33–42.
[6] R. Langer, L. Brown, E. Edelman, Controlled release and magnetically modulated release systems for macromolecules, Methods Enzymol. 112 (1985) 399–422.
[7] T. Parker, V. Dave, R. Falotico, Polymers for drug eluting stents, Curr. Pharm. Des. 16 (2010) 3978–3988.
[8] Y. Otsuka, S. Saito, M. Nakamura, H. Shuto, K. Mitsudo, Comparison of pharmacokinetics of the limus-eluting stents in Japanese patients, Catheter. Cardiovasc. Interv. 78 (7) (2011) 1078–1085.
[9] C.W. Hwang, D. Wu, E.R. Edelman, Physiological transport forces govern drug distribution for stent-based delivery, Circulation 104 (5) (2001) 600–605.
[10] K.R. Kamath, J.J. Barry, K.M. Miller, The Taxus drug-eluting stent: a new paradigm in controlled drug delivery, Adv. Drug Deliv. Rev. 58 (3) (2006) 412–436.
[11] V.B. Kolachalama, E.G. Levine, E.R. Edelman, Flow amplifies stent-based drug deposition in arterial bifurcations, PLoS One 4 (12) (2009) e8105.
[12] CE Marked in 2006 and distributed in the EU by Eurocor GmbH, http://www.eurocor.de/products/genius_magic/product_information/.
[13] A.R. Tzafriri, A.D. Levin, E.R. Edelman, Diffusion-limited binding explains binary dose response for local arterial and tumour drug delivery, Cell Prolif. 42 (2009) 348–363.
[14] A.D. Levin, M. Jonas, C.W. Hwang, E.R. Edelman, Local and systemic drug competition in drug-eluting stent tissue deposition properties, J. Control. Release 109 (1–3) (2005) 236–243.
[15] M. Horner, S. Joshi, V. Dhruva, S. Sett, S.F.C. Stewart, A two-species drug delivery model is required to predict deposition from drug-eluting stents, Cardiovasc. Eng. Technol. 1 (2010) 225–234.
[16] J.L. Fulton, G.S. Deverman, C.R. Yonker, J.W. Grate, J. De Young, J.B. McClain, Thin fluoropolymer films and nanoparticle coatings from the rapid expansion of supercritical carbon dioxide solutions with electrostatic collection, Polymer 44 (2003) 3627–3632.
[17] R. Gurny, E. Doelker, N.A. Peppas, Modelling of sustained release of water-soluble drugs from porous, hydrophobic polymers, Biomaterials 3 (1) (1982) 27–32.
[18] M. Cilingiroglu, J. Elliott, P. Sangi, H. Matthews, F. Tio, B. Trauthen, J. Elicker, S.R. Bailey, In vivo evaluation of a biolimus eluting nickel titanium self expanding stent with overlapping balloon expandable drug eluting and bare metal stents in a porcine coronary model, EuroIntervention 4 (4) (2009) 534–541.
[19] G.J. Wilson, B.A. Huibregtse, E.A. Stejskal, J. Crary, R.M. Starzyk, K.D. Dawkins, J.J. Barry, Vascular response to a third generation everolimus-eluting stent, EuroIntervention 6 (4) (2010) 512–519.
[20] A.V. Finn, F.D. Kolodgie, J. Harnek, L.J. Guerrero, E. Acampado, K. Tefera, K. Skorija, D.K. Weber, H.K. Gold, R. Virmani, Differential response of delayed healing and persistent inflammation at sites of overlapping sirolimus- or paclitaxel-eluting stents, Circulation 112 (2005) 270–278.
[21] B. Balakrishnan, J.F. Dooley, G. Kopia, E.R. Edelman, Intravascular drug release kinetics dictate arterial drug deposition, retention, and distribution, J. Control. Release 123 (2) (2007) 100–108.
[22] Data on file at Micell Technologies, Inc.
[23] Y. Minami, H. Kaneda, M. Inoue, M. Ikutomi, T. Morita, T. Nakajima, Endothelial dysfunction following drug-eluting stent implantation: a systematic review of the literature, Int. J. Cardiol. (Mar 27, 2012) (Epub ahead of print).
[24] P. Macheras, A. Iliades, Modeling in Biopharmaceutics, Pharmacokinetics and Pharmacodynamics, II, Springer Science and Business Media, Inc. Publishers, New York, 2006.
[25] M.G. Attur, R. Patel, G. Thakker, P. Vyas, D. Levartovsky, P. Patel, S. Nagvi, R. Raza, K. Patel, D. Abramson, G. Bruno, S.B. Abramson, A.R. Amin, Differential anti-inflammatory effects of immunosuppressive drugs: cyclosporine, rapamycin and FK-506 on inducible nitric oxide synthase, nitric oxide, cyclooxygenase-2 and PGE2 production, Inflamm. Res. 49 (1) (2000) 20–26.
[26] K.L. Ma, Z. Xiong, S.H. Ruan, H. Powis, J.F. Moorhead, Z. Varghese, Anti-atherosclerotic effects of sirolimus on human vascular smooth muscle cells, Am. J. Physiol. Heart Circ. Physiol. 292 (2007) H2721–H2728.
[27] T. Xi, R. Gao, B. Xu, L. Chen, T. Luo, J. Liu, Y. Wei, S. Zhong, In vitro and in vivo changes to PLGA/sirolimus coating on drug eluting stents, Biomaterials 31 (2010) 5151–5158.
[28] S. Garg, P.W. Serruys, Coronary stents looking forward, J. Am. Coll. Cardiol. 56 (10 S) (2010) S43–S78.